RSC Sustainability

ROYAL SOCIETY OF CHEMISTRY

PAPER

View Article Online
View Journal | View Issue

Cite this: *RSC Sustainability*, 2024, **2**, 2532

On the synthesis of biorefineries for high-yield isobutanol production: from biomass-to-alcohol experiments to system level analysis†

Arthur E. Pastore de Lima, [a] Jason Coplien, [bc] Larry C. Anthony,[d] Trey K. Sato, [b] Yaoping Zhang, ‡[b] Steven D. Karlen, [bc] Chris Todd Hittinger [bce] and Christos T. Maravelias *[af]

The production of isobutanol from lignocellulose has gained attention due to its favorable physical and chemical properties. The use of lignocellulosic biomass as a feedstock to produce isobutanol has substantial sustainability benefits, but the biological conversion to isobutanol faces challenges, such as low yields and by-product formation. In this work, we demonstrate the high-yield production of isobutanol through microbial fermentation of pulp hydrolysates. Three hydrolysates are produced from poplar, sorghum, and switchgrass using pretreatment based on γ-valerolactone. Furthermore, we synthesize a biomass-to-isobutanol biorefinery and perform technoeconomic analysis of three resulting processes using experimental results obtained from an engineered yeast strain which consumes most of the glucose available in the hydrolysate and produces isobutanol at 89–94% theoretical yields. The corresponding minimum fuel selling price (MFSP) is $14.40–$16.01 per gasoline gallon equivalent, with the sorghum-based biorefinery resulting in the lowest price. We identify that solvent/biomass ratio during pretreatment and enzyme loading during hydrolysis have the greatest impact on the MFSP; improvements in these parameters can reduce the MFSP by 46%.

Received 3rd June 2024
Accepted 2nd August 2024

DOI: 10.1039/d4su00283k

rsc.li/rscsus

Sustainability spotlight

Biological fermentation is a promising technology for the sustainable production of fuels and chemicals such as isobutanol. However, fermentation may exhibit low yields and significant by-product formation resulting in complex and expensive processes. Our interest is in experimentally producing isobutanol at high yields from lignocellulosic biomass with low by-product formation and identifying key areas of improvement to reach an economically competitive biorefinery. Remarkably, we achieved isobutanol yields as high as 94% of the theoretical maximum. Our technoeconomic analysis indicates that improvements in the pretreatment and hydrolysis steps would significantly impact the economic viability of the process. Our work emphasizes the importance of the following UN sustainable development goals: industry, innovation, and infrastructure (SDG 9), climate action (SDG 13).

1 Introduction

Isobutanol (IBA) has gained attention in recent years, as a potential lignocellulosic biofuel, due to its superior properties compared to ethanol. IBA has a higher energy density, lower vapor pressure and better compatibility with the existing fuel infrastructure, and is less corrosive, making it a versatile option for use as a fuel or additive.[1] Furthermore, IBA has a wide range of industrial applications as a solvent and chemical intermediate. It is used to produce esters[2] and ketones,[3] and it can be upgraded to isobutene,[4] jet fuel, and diesel.[5,6]

IBA can be produced by biological fermentation where a microorganism, such as a bacterium or yeast, converts sugars to IBA. The use of sustainable lignocellulosic feedstocks, which can be widely available at low cost and produced on lands that are not used for food production,[7,8] to produce the hydrolysate for the biological conversion is a green route to produce IBA.

Lignocellulosic biomass is mainly composed of cellulose, hemicellulose, and lignin.[9] A pretreatment step disrupts (and often removes some of) the lignin structure, removes or destroys microbial inhibitors, and increases the accessibility of cellulose

[a]*Andlinger Center for Energy and the Environment, Princeton University, Princeton, NJ 08544, USA. E-mail: maravelias@princeton.edu*

[b]*DOE Great Lakes Bioenergy Research Center, University of Wisconsin, Madison, WI 53726, USA*

[c]*Wisconsin Energy Institute, University of Wisconsin-Madison, Madison, Wisconsin 53726, USA*

[d]*IFF, Health and Biosciences, Wilmington, DE, USA*

[e]*Laboratory of Genetics, J. F. Crow Institute for the Study of Evolution, Center for Genomic Science Innovation, University of Wisconsin-Madison, Madison, WI 53726, USA*

[f]*Department of Chemical and Biological Engineering, Princeton University, Princeton, NJ 08544, USA*

† Electronic supplementary information (ESI) available. See DOI: https://doi.org/10.1039/d4su00283k

‡ Deceased.

and hemicellulose for more efficient hydrolysis into fermentable monomeric sugars. During hydrolysis, enzymes depolymerize the cellulose into glucose (a C_6 sugar) and the hemicellulose into C_6 and C_5 sugars, such as glucose and xylose, respectively. Recently, the use of γ-valerolactone (GVL) in biomass fractionation processing has been proposed as a potential alternative to traditional pretreatment and enzymatic hydrolysis methods.[10,11] GVL is a biomass-derived renewable solvent[12] capable of completely solubilizing lignocellulosic biomass at 165 °C.[13] GVL has a boiling point of 207 °C and a low vapor pressure, which make it a solvent that can be used at elevated temperatures (>150 °C). In addition, the use of GVL allows the fractionation of the cellulose and hemicellulose biomass fractions into separate streams without additional processing steps.[14]

Next, the sugars serve as substrates for microorganisms to metabolize into chemicals and fuels, such as IBA. Most microorganisms have a low tolerance to IBA and are unable to grow in fermentation broths containing more than 1 wt% IBA.[15–17] To increase the IBA yield in biological fermentation processes, different techniques have been proposed for the *in situ* removal of IBA.[18] For instance, a vacuum flash unit can be used to remove IBA-rich vapors, keeping the IBA concentration in the broth below toxic levels.[19] Finally, the broth and the IBA-rich vapors are purified to obtain IBA.

In addition to addressing the toxicity of elevated IBA concentrations, genetic engineering focuses on increasing the IBA yields and titers obtained from glucose (and other sugars) by microorganisms such as *Saccharomyces cerevisiae*,[20–23] *Escherichia coli*,[24–26] and others.[7,27–29] Liu *et al.* found that an engineered *Zymomonas mobilis* IBA-producing strain was able to produce 6 g L^{-1} of IBA after consuming 30.6 g L^{-1} of glucose (~50% of the theoretical maximum) in rich medium with glucose.[27] Minty *et al.* produced 1.88 g L^{-1} of IBA from pretreated corn stover using a microbial consortium of fungal *Trichoderma reesei* and bacterial *E. coli*, achieving 62% of the theoretical yield.[29] Jung *et al.* produced 23 g L^{-1} of IBA (~34% of the theoretical maximum) using engineered *Enterobacter aerogenes* from sugarcane bagasse.[28]

Microbes typically produce other fermentation by-products, potentially increasing the complexity of the IBA recovery step(s). Ethanol is the most common by-product obtained during IBA production.[7] Some of the other by-products include 2-methyl-1-butanol,[21] hexanol,[30] lactate, glycerol, and succinate.[31] However, Bastian *et al.* were able to produce IBA at 100% of the theoretical maximum yield using an engineered strain of *E. coli* under anaerobic fermentation.[32]

A few authors have performed technoeconomic analysis (TEA) of IBA biorefineries.[19,33,34] Tao *et al.* studied the use of corn stover as the feedstock to produce IBA from glucose and xylose at 85% of the theoretical maximum yield, obtaining a minimum fuel selling price (MFSP) of $3.62/gasoline gallon equivalent (GGE).[34] The MFSP can be viewed as the price required so that the total revenues are equal to the total costs of the biorefinery. Roussos *et al.* assumed yields of 85% (or 90%) of the theoretical maximum from glucose and xylose and obtained an MFSP of $6.53 GGE^{-1} (or $4.14 GGE^{-1}, respectively) for IBA using corn stover as the feedstock.[19] Note that these works assumed that xylose is converted at yields comparable to glucose, where the high xylose-to-IBA yields were not verified experimentally. Recently, Pastore de Lima *et al.* developed a biorefinery for the co-production of IBA and ethanol from switchgrass based on experimental data. A hybridized yeast strain able to ferment glucose from ammonia fiber expansion (AFEX) hydrolysates was used to produce IBA and ethanol at high yields. An MFSP of $11.43 GGE^{-1} for the alcohols was determined, where lower hydrolysis enzyme loadings and the ability to ferment xylose had the greatest potential to reduce the MFSP.[35] In this work, we focus on an entirely different system.

We first demonstrate the high-yield production of IBA as the main product from cellulose fibers isolated from poplar, sorghum, and switchgrass pretreated by a GVL-based process, reaching more than 90% of the theoretical maximum. Then, we synthesize a biomass-to-IBA biorefinery with emphasis on the fermentation and separation processes. During fermentation, the *in situ* IBA removal is modeled using vacuum flash to avoid IBA concentrations in the broth reaching levels that are toxic to microorganisms. Finally, we perform technoeconomic analysis of the biorefinery based on the experimental data obtained and perform sensitivity analysis to provide further insights into improvements that could result in an economically attractive process. The solvent/biomass ratio during pretreatment and enzyme loadings during hydrolysis have the greatest impact on the minimum fuel selling price.

Importantly, our system offers improvements in terms of sustainability compared to other experimental-based lignocellulosic biorefineries.[35] First, the GVL used in this study has low toxicity and is a renewable and green solvent[36] when compared with ammonia used during AFEX. Second, the high-yield production of IBA with minimal ethanol production allows for a less complex downstream separation process and thus lower energy demand. Finally, the study of bioenergy crops such as poplar is associated with higher greenhouse gas mitigation potential[37] and increased biodiversity[38] compared with switchgrass.

2 Results and discussion

2.1. Pretreatment and hydrolysis

Three lignocellulosic plant feedstocks are used in this study: poplar, sorghum, and switchgrass. The feedstocks are fractionated using GVL to obtain cellulose fibers, which are hydrolyzed by enzymes to generate a stream rich in glucose. Approximately 28–30 mL of hydrolysates are obtained from 6.5–7.1 g of cellulose fibers. The glucose concentrations in the resulting hydrolysates are between 101–114 g L^{-1}, where the glucan-to-glucose yields are 86–90%. Additional details of the pretreatment and hydrolysis results obtained for each feedstock are given in Table S1 in the ESI.†

2.2. Fermentation

An engineered *Saccharomyces cerevisiae* strain, BTX1858, from Butamax Advanced Biofuels, LLC, is a high-yielding starch

Table 1 Initial glucose concentration in hydrolysates produced from GVL-purified cellulose fibers and IBA concentrations obtained from fermentation of the hydrolysates. IBA yields are shown as a fraction of the theoretical maximum (0.41 g g^{-1} of glucose)

Biomass	Glucose initial conc. (g L^{-1})	IBA conc. (g L^{-1})	IBA yield
Poplar	51.4 ± 2.9	18.7 ± 1.7	89% ± 3%
Sorghum	57.7 ± 1.1	22.3 ± 2.4	94% ± 12%
Switchgrass	54.4 ± 1.1	20.1 ± 1.1	90% ± 6%

isobutanologen. Previously, we determined that BTX1858 produces 0.01 g L^{-1} of IBA from ~60 g L^{-1} of glucose in AFEX-pretreated switchgrass hydrolysate (ASGH), while producing up to 15 g L^{-1} of IBA from rich lab medium containing the same concentration of glucose.[35] This result, coupled with the lack of growth and glucose consumption in ASGH, suggests that chemical compounds in ASGH inhibited glucose conversion by the BTX1858 strain. A process using GVL as the solvent fractionates biomass into two separate streams; one is rich in cellulose, while the other is reach in lignin, hemicellulose, and soluble metabolites (see Section 4.2). Since the majority of lignocellulose-derived inhibitors come from the lignin, hemicellulose, and soluble metabolites stream (including ferulate, *p*-coumarate, and phenolic aldehydes),[39] we hypothesize that the BTX1858 strain would produce higher titers and yields of IBA from the cellulose stream of GVL-deconstructed biomass than what was seen with the single combined AFEX-deconstructed stream. Therefore, we generated and tested hydrolysates from GVL-purified cellulose fibers (Section 4.3).

The GVL-deconstructed hydrolysates from the three feedstocks were inoculated with the BTX1858 yeast strain. The cultures were then overlayed with oleyl alcohol (a solvent separation process to mimic the vacuum process used in the biorefinery model, see Section 4.4) and fermented anaerobically for 48 h. The BTX1858 strain produced 18.7–22.3 g L^{-1} of IBA at 89–94% of the maximum theoretical yield (Table 1). The isobutanologenic strain used nearly all the glucose and produced only small amounts of ethanol. See Table S1 in the ESI† for details.

2.3. Process synthesis

We synthesize a biomass-to-IBA biorefinery (Fig. 1) and study the use of poplar, sorghum, and switchgrass as feedstocks. The biomass is deconstructed using a GVL-based biomass fractionation process (GVL block), which produces three streams: (1) solid cellulose pulp sent to hydrolysis (HYD);[40] (2) solid residue consisting of lignin and unconverted glucan and xylan, which is sent to the combustor and boiler (CB);[10] and (3) liquid residue rich in xylose, which is sent to wastewater treatment (WWT).[10] Note that GVL is recycled within the block (see Section S3.2 in the ESI†). During hydrolysis, the pulp is converted into a glucose-rich stream that is sent to the fermentation block (FERM); the remaining unconverted solids from the pulp are sent to the CB block. In the FERM block, strain BTX1858 converts the glucose into IBA following the yields obtained experimentally (Table 1). The fermentation broth is sent to the separation block (SEP) to recover IBA. The residual stream (stillage) is sent to the WWT block, where biogas is produced from carbon-rich residues, such as unconverted sugars (glucose and xylose) and fermentation by-products. The biogas and the solids collected from GVL and HYD blocks are used to produce heat. Excess heat is used for electricity production in the turbogenerator block (TBG), and any surplus of electricity is sold to the grid. Fig. 1 shows the detailed flows in the biorefinery using poplar as feedstock. Section S2 in the ESI† contains similar figures for the biorefineries using sorghum and switchgrass, and the carbon balance of the biorefinery for each feedstock.

Each block in the process is characterized by cost, energy (*i.e.*, heat and electricity) requirements, and conversion parameters. The baseline values for the conversion parameters of the GVL and HYD blocks are based on the experimental results and mass balances for these processes, while the cost and energy demand parameters are calculated from the literature[10,40–43] after adjustments to account for the values of experimental operating parameters used in this work (*e.g.*, solvent/biomass ratio and enzyme loading – see Sections 4.2 and 4.3). The parameter values for the WWT, CB, and TBG blocks are estimated from the literature[41,44,45] and are given in Tables S4 and S5 in the ESI.†

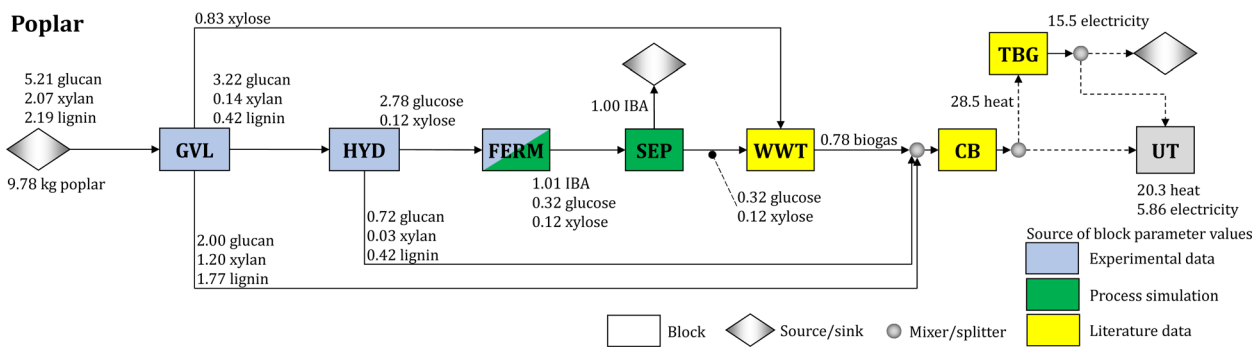

Fig. 1 Block flow diagram of the baseline biomass-to-IBA biorefinery, using poplar as feedstock. Mass flows are in units of kg kg^{-1} of IBA produced, and heat and electricity flows are in units of kWh kg^{-1} of IBA. Abbreviations – CB: combustor and boiler, FERM: fermentation, GVL: γ-valerolactone, HYD: hydrolysis, SEP: separations, TBG: turbogenerator, UT: utilities, WWT: wastewater treatment.

Parameters for the FERM and SEP blocks are determined based on a process simulation developed in Aspen Plus V11 (Aspen Technology Inc.). The FERM block uses vacuum stripping to remove IBA during fermentation and maintain a low IBA concentration in the broth. The SEP block uses two distillation columns and a decanter to break the water–IBA azeotrope and purify the IBA (see Section 4.4). The process simulation results are used to estimate the cost and energy demand parameters of the FERM and SEP blocks. Furthermore, the SEP block is designed to recover 99% of the inlet IBA at 99.5% purity. The values of all estimated parameters are given in Tables S4 and S5 in the ESI.†

The synthesis of the biorefinery is based on an optimization model[35,44,45] that includes material and energy balances across all the major blocks. We minimize the cost to produce one kg of IBA. The complete mathematical formulation is presented in Section S4 in the ESI.†

2.4. Technoeconomic analysis

We determine that the MFSP of IBA for the baseline design is \$16.01, \$14.40, and \$15.55 GGE^{-1} using poplar, sorghum, and switchgrass, respectively. Fig. 2 summarizes the cost contributors of the biorefinery for each feedstock. In all three systems, the HYD and GVL blocks are the major cost contributors (36.6–37.4% and 26.7–32.1% of the MFSP, respectively), followed by feedstock purchasing (17.8–19.0%). The biomass-to-IBA yields are 0.102, 0.136, and 0.125 kg IBA per kg of biomass using poplar, sorghum, and switchgrass, respectively.

The total estimated heat and electricity demands of the biorefinery using poplar as feedstock are 20.3 kWh and 5.9 kWh kg^{-1} of IBA produced, respectively. Furthermore, the use of poplar results in higher flows of glucan and lignin sent to the CB block compared to the use of sorghum and switchgrass, as less glucan is converted into glucose during pretreatment and hydrolysis. This results in a high revenue obtained from surplus electricity sold to the grid (21.1% of the MFSP), but a low glucose yield after hydrolysis from the biomass (0.284).

The use of switchgrass as feedstock leads to a high glucan retention in the cellulose fibers (~93%) compared to the use of other feedstocks (see Fig. S2 in the ESI†) despite the low glucan content of switchgrass (42.5%). Therefore, a lower fraction of solids is used for heat production, leading to a low revenue from surplus electricity sales (14.1% of the MFSP). The biomass-to-glucose yield is 0.343. The heat and electricity demands are 18.2 kWh and 5.7 kWh kg^{-1} of IBA, respectively.

Finally, the use of sorghum leads to the lowest MFSP among the studied feedstocks (see Fig. S3 in the ESI†). During pretreatment, 82.1% of the glucan in the biomass is retained in the cellulose fibers, and 90.3% of the retained glucan is converted into glucose during hydrolysis, which results in the highest biomass-to-glucose yield (0.356). Furthermore, during fermentation, the hydrolysate obtained from sorghum showed the highest glucose-to-isobutanol conversion (Table 1), resulting in the highest overall biomass-to-isobutanol yields. A revenue equivalent to 12.3% of the MFSP is obtained from surplus electricity sales, and the estimated heat and electricity demands are 17.2 kWh and 5.1 kWh kg^{-1} of IBA, respectively.

Note that grasses like sorghum and switchgrass are typically easier to be pretreated than woods like poplar. This is due to a combination of factors: (1) wood fibers are generally longer than grass fibers and tend to get entangled during processing; (2) lignin in grasses is more water soluble than the wood lignin, making them easier to be removed; and (3) grasses have ferulate and diferulates on the hemicellulose that breakdown easily in acidic conditions and aid the biomass processing.

2.5. Sensitivity analysis

We select sorghum as the feedstock to study the change in the MFSP. We consider the following parameters: (1) GVL/biomass mass ratio in biomass fractionation, (2) enzyme loading in hydrolysis, (3) cost of the FERM block, and (4) heat demand of the SEP block. We solve updated instances of the optimization model using updated block parameters calculated using the new values of parameters (1)–(4). More details can be found in Section S5 in the ESI.† The GVL/biomass ratio affects equipment sizes in the GVL block, impacting both capital and operating costs, and heat requirement, which is significant in the GVL block.

The enzyme loading during hydrolysis affects the size of equipment, the energy requirement, and raw material purchasing associated with the enzyme production within the HYD block. Note that the impact of enzyme production represents nearly 90% of the total costs in the HYD block due to the high enzyme loading used in the experiments (133 mg protein

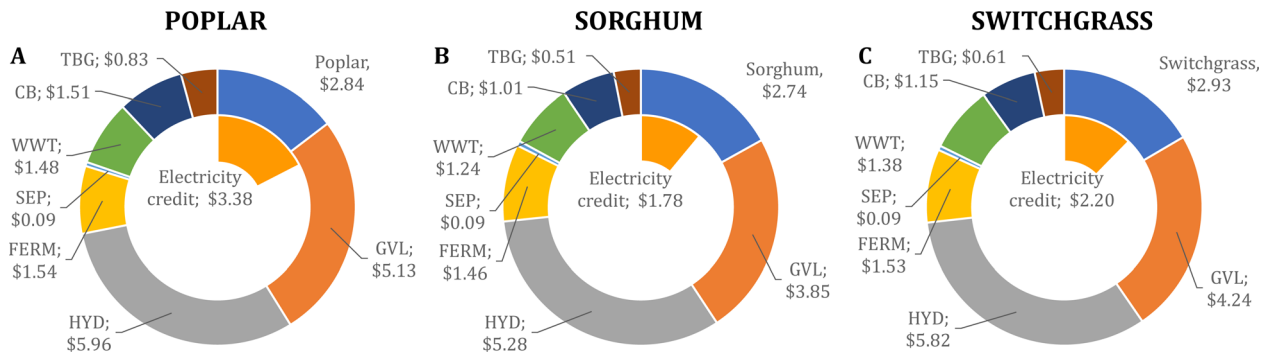

Fig. 2 Cost contributions in the baseline biorefinery using (A) poplar, (B) sorghum, and (C) switchgrass. Values shown are based on 1 GGE of IBA produced. The MFSP using each biomass is \$16.01, \$14.40, and \$15.55 GGE^{-1} for poplar, sorghum, and switchgrass, respectively.

g^{-1} cellulose). The use of lower enzyme loadings have been considered in other works.[35,41,46] For instance, 93 mg protein g^{-1} cellulose were used during the hydrolysis of AFEX-pretreated switchgrass in experiments to co-produce isobutanol and ethanol.[35] Humbird *et al.* considered the use of ~20 mg protein g^{-1} cellulose in NREL studies for ethanol biorefineries using diluted acid as the pretreatment process.[41]

Improvements in the cost parameter of the FERM block can be achieved by implementing different strategies for the *in situ* removal of isobutanol from the fermentation broth. Similarly, the heat requirement of the SEP block can be improved by alternative separation technologies that do not use distillation or employ heat integration. For instance, based on simulation results, the heat required in the baseline design proposed for the FERM and SEP blocks in Section 4.4 can be reduced by 43% *via* heat integration.

In Fig. 3A, we show the MFSP as a function of the GVL/biomass ratio in the GVL block and the enzyme loading in the HYD block. The MFSP decreases to \$9.74 GGE^{-1} if the enzyme loading is reduced to 20 mg protein g^{-1} cellulose (~85% reduction compared to the experimental value), which is the value considered in NREL studies.[41] The MFSP can be further reduced to \$7.72 GGE^{-1} if the GVL/biomass ratio can be decreased to 4.0 (44% reduction), representing a combined 46% MFSP decrease (Fig. 4A). Note that for these results it is assumed that the conversion parameters in the GVL and HYD blocks are not impacted by the reduction in the GVL/biomass ratio and enzyme loading.

Fig. 3B shows the impact of the FERM cost and SEP heat requirement on the MFSP. First, the MFSP decreases by \$0.88 GGE^{-1} if the costs associated with FERM are reduced to 40% of the baseline value. In the FERM block, the compressors have the highest cost contribution to the FERM cost, and therefore an alternative design (*e.g.*, solvent extraction, pervaporation) would be required to remove isobutanol from the broth and achieve such a cost reduction. Furthermore, an additional \$0.52 GGE^{-1} is saved if the heat requirement in the SEP block is reduced to 40% of the original value. Finally, the combination of the improvements in the GVL, HYD, FERM, and SEP blocks have the potential to reduce the MFSP to \$6.33 GGE^{-1} (Fig. 4A).

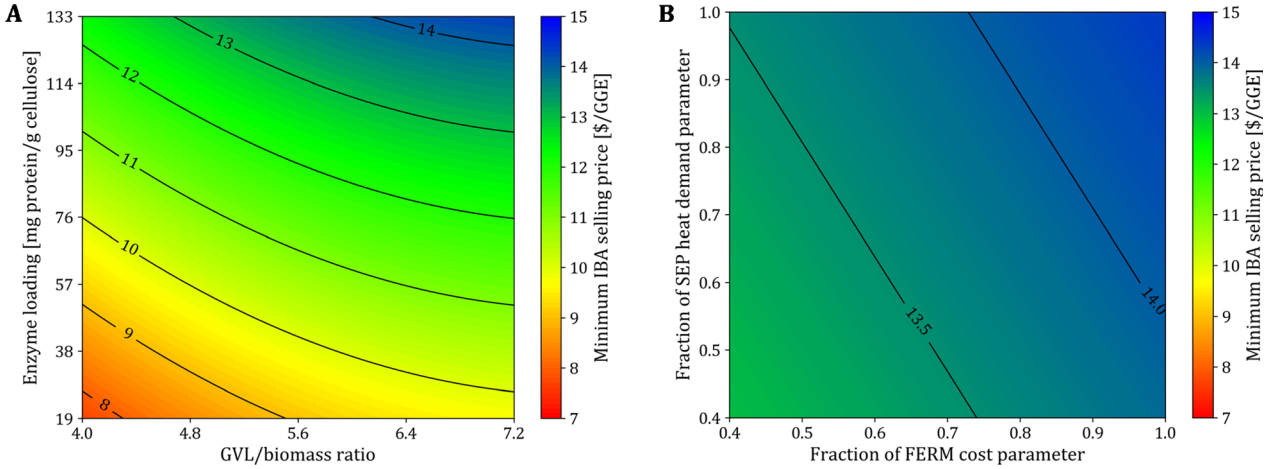

Fig. 3 MFSP of the biorefinery using sorghum as a function of (A) GVL/biomass mass ratio during pretreatment and enzyme loading during hydrolysis; and (B) cost parameter of FERM block and heat demand parameter of SEP block; the axis values are fractions of the base case parameter values.

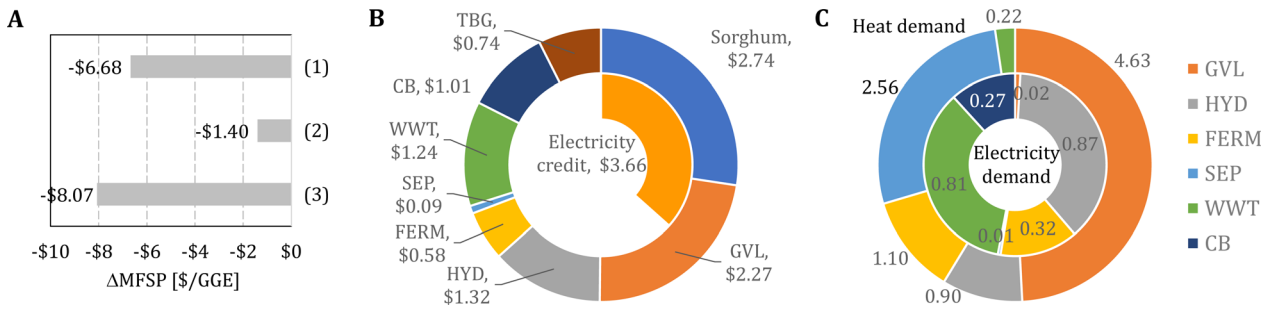

Fig. 4 Sensitivity analysis for the biorefinery using sorghum. (A) Change in the MFSP based on three cases: (1) improvements in the pretreatment (GVL/biomass ratio of 4.0) and hydrolysis (enzyme loading of 20 mg protein g^{-1} cellulose), (2) improvements in the designs of the FERM (40% of the baseline cost parameter) and SEP block (40% of the baseline heat demand parameter), and (3) the combination of the improvements in (1) and (2). (B) Cost contributors of case (3); costs shown are based on 1 GGE of IBA produced. (C) Energy demand breakdown in case (3); values shown are in kWh GGE^{-1}.

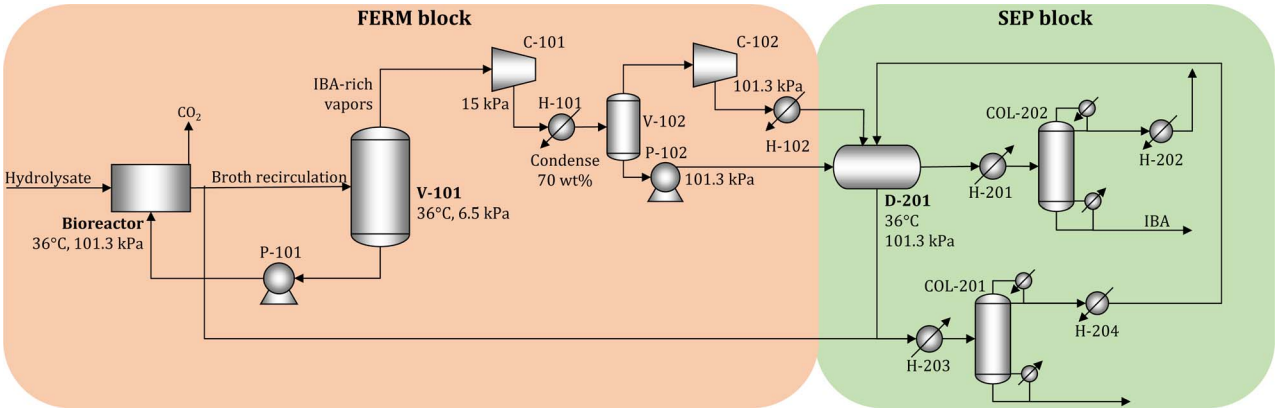

Fig. 5 Process flow diagram of the FERM and SEP blocks simulated in Aspen Plus V11.

In Fig. 4B and C, we show, respectively, the cost contributors and the energy demand of the biorefinery considering the following improvements simultaneously: (1) a 4.0 GVL/biomass mass ratio, (2) a 20 mg protein g^{-1} cellulose enzyme loading for hydrolysis, (3) FERM cost 40% of its baseline value, and (4) a SEP heat requirement equal to 40% of its baseline value. First, the feedstock purchasing represents the highest cost contributor (43% of the MFSP), followed by the GVL (36%) and HYD (21%) blocks, which are now much cheaper compared to the baseline design (see Fig. 2B) due to the reduced GVL/biomass ratio and enzyme loading, respectively. Furthermore, there is a two-fold increase in the electricity credit compared to the baseline design, representing nearly 58% of the MFSP of \$6.33 GGE^{-1}. Finally, the GVL and SEP blocks have the most significant heat requirements, representing 49% and 27% of the 9.41 kWh GGE^{-1} of consumed heat. The electricity demand is 2.29 kWh GGE^{-1} driven by the HYD (38%) and WWT (35%) blocks.

2.6. Remarks

Different biomass fractionation methods based on GVL have been proposed.[13,14] For instance, GVL can completely solubilize the biomass and produce a single stream containing the glucose and xylose sugars, avoiding the need for the enzymatic hydrolysis step. However, inhibitors and other toxic components can also be present in the stream and would significantly affect microorganism growth and isobutanol production during fermentation. The biomass fractionation method used in this work, on the other hand, removes most inhibitory components from the resulting cellulose fibers (not solubilized by GVL), generating a cleaner hydrolysate that is more suitable for the microorganism growth during fermentation.

Nevertheless, relatively high solvent/biomass ratio and enzyme loadings were required for biomass pretreatment and hydrolysis, so new studies aiming at improving these processes are needed. Finally, residue valorization strategies (*e.g.*, stillage or lignin valorization) may be implemented to improve the economics of the biorefinery. For instance, strain engineering advances may allow the yeast to convert xylose to isobutanol, and thus the xylose-rich residue stream may be converted into additional isobutanol, potentially reducing the MFSP.

3 Conclusions

We study the production of IBA from glucose in lignocellulosic biomass hydrolysates pretreated using a GVL-based technology. We consider the use of poplar, sorghum, and switchgrass as the feedstocks. The two grasses, sorghum and switchgrass, showed high glucan retention in the cellulose pulps after pretreatment (82% and 91%, respectively) while poplar retained only ~63% of the initial glucan. After hydrolysis of the cellulose pulps, we employ a yeast strain (BTX1858) for fermentation, consuming most glucose and producing isobutanol at yields of ~90% of the theoretical maximum. Xylose remains unconverted, and only very small amounts of ethanol are produced.

We synthesize a biomass-to-IBA biorefinery based on the results using the BTX1858 strain to produce IBA at a cost of \$14.40–\$16.01 GGE^{-1}. Our analysis indicates that the GVL and HYD blocks have the highest cost contributions for the baseline designs due to the high solvent/biomass ratio and enzyme loadings used in our experiments. Sensitivity analysis, based on the biorefinery that uses sorghum as feedstock, indicates that the GVL/biomass ratio during pretreatment and enzyme loading during hydrolysis are the most important factors in terms of the total biorefinery cost. Improvements in these parameters can reduce the MFSP to \$7.72 GGE^{-1}. Therefore, new studies focused on optimizing these parameters are important for obtaining a cost competitive biorefinery.

4 Methods

4.1. Biomass description and preparation

NM6 hybrid poplar (*Populus maximowiczii X nigra*) planted in 2013 and harvested in 2018 from Oregon, WI was debarked, chipped, dried, and fractionated to pass through a 5 mm round hole on a shaker table. The energy sorghum (*Sorghum bicolor*) and "Cave-In-Rock" switchgrass (*Panicum virgatum*) were grown and harvested in 2014 and 2016, respectively, from Arlington Agricultural Research Station[47] in Arlington, Wisconsin. Sorghum and switchgrass were harvested with a John Deere 7350 Self-propelled forage harvester/chopper, dried and fractionated to pass through a 5 mm round hole on a shaker table. Carbohydrate compositions for the milled feedstocks were

determined by cell wall isolation, acid hydrolysis, solvent extraction and gas chromatography-mass spectrometry as previously described.[48]

4.2. GVL pretreatment

The GVL-fractionation process is carried out in a 2 L, flow-through, Parr reactor. The process is optimized to separate the cellulose fibers from the hemicellulose and lignin.[40,49] Milled biomass (150 g) is suspended in a 3 : 1 mixture of GVL and water containing 0.1 M of sulfuric acid (H_2SO_4) at a GVL/dry biomass mass ratio of 7.2. The water and acid content aids in solubilizing the hemicellulose, while GVL extracts the lignin. Lignin and hemicellulose are extracted at 120 °C, and most of the cellulose is preserved and left as fibers, which are easily separated from the GVL/water extract. The fibers are washed with fresh water to remove excess GVL and other water-soluble microbial growth inhibitors.

4.3. Hydrolysis and fermentation

Glucan and moisture contents of the biomass pulps are determined prior to hydrolysis (Table S1†). Moisture content is measured by an Ohaus MB35 Moisture Analyzer (Ohaus Corporation, Parsippany, NJ), and the glucan content is determined by NREL protocol.[50]

Small-scale hydrolysis was performed in 85 mL Nalgene Oak Ridge centrifuge tubes (Thermo Scientific, Cat#: 3118-0085) with a total loading of 50 g and 7% glucan loading. The GVL-pretreated pulp (~6.5–7.1 g) is loaded into the tube, followed by water and 5 mL 1 M phosphate buffer (127.16 g KH_2PO_4 per L and 11.32 g K_2HPO_4 per L). The tubes are autoclaved at 121 °C for an hour. After cooling down to ~50 °C, cellulase (NS 22257) and xylanase (NS 22244) from Novozymes are added at concentration of 120 and 13 mg protein g^{-1} glucan, respectively. Hydrolysis is carried out at 50 °C for 7 days. After centrifugation, hydrolysates are adjusted to a pH of 5.8 by adding 12 N NaOH and then filtered using Nalgene 50 mL filter unit (0.2 μ pore size, Nalgene, Cat#: 564-0020).

The fermentation experiments in Table 1 were carried out in a respirometer system as described previously[35] after diluting the hydrolysates 1 : 1 with water and supplementing them with 5 g L^{-1} of yeast extract. Dilution and supplementation were done to maximize strain performance.[35] The starter cultures of BTX1858 were grown in SD media aerobically overnight and then inoculated into 4 mL of each hydrolysate in sterile 60 mL Wheaton serum bottles with initial OD600 values of 0.5. The media were overlayed with 4 mL of oleyl alcohol. After the fermentations were completed, the media and oleyl alcohol were separated by centrifugation, and both phases were analyzed by HPLC-RID and GC/MS to measure the concentrations of glucose, xylose, IBA, and other end products as described previously.[20] IBA from both phases were combined to obtain the final IBA concentration.

4.4. Process simulation

We simulate the unit operations of the FERM and SEP blocks using Aspen Plus V11 (Aspen Technology Inc.) to obtain accurate estimates of the cost and energy requirements. In the simulations, we consider that the biorefinery processes 2000 Mg day^{-1} of dry biomass. The process flow diagram is shown in Fig. 5.

The pulp hydrolysate is processed in 12 parallel bioreactors, each processing 39.1–44.4 m^3 h^{-1} of hydrolysate (depending on the feedstock). We employ vacuum stripping to remove IBA *in situ* from the broth.[19,51] Part of the broth is sent to a vacuum flash (V-101) operating at 6.5 kPa and 36 °C, where the vapor stream rich in IBA is removed and the liquid stream returns to the bioreactor. The fraction of broth sent to V-101 is adjusted to maintain the IBA concentration in the broth at 1% (weight), where the remaining broth is sent to the beer column (COL-201). The IBA-rich vapor is compressed (C-101, C-102) and liquefied (H-101, H-102), and sent to a decanter (D-201) to obtain two liquid phases. The water-rich phase is mixed with broth and sent to COL-201, where water is removed at the bottom. The column is designed to allow the loss of 1% of the produced IBA. The distillate stream contains most of the inlet IBA and is recycled to D-201. The IBA-rich phase from D-201 is sent to another distillation column (COL-202), where IBA is recovered with 99.5% purity at the bottom stream and the distillate is recycled to D-201. The details of the economic assumptions, including cost and energy demand estimates, are given in Section S3 in the ESI.†

4.5. Process synthesis

The optimization model of the biomass-to-isobutanol biorefinery (Fig. 1) is formulated in GAMS (36.1.0). Each block is described by the following parameters: (1) cost, including both capital and operating costs (\$ kg^{-1}); (2) energy demand, including power and heat required to operate the unit (kWh kg^{-1}); and (3) conversion parameters for all (input, output) pairs of materials with positive conversion. The conversion parameters describe the conversion of components from the inlet stream into components in the outlet streams of the block. The complete mathematical formulation, the details of parameter value estimation, and the list of used parameter values is presented in Sections S3 and S4 in the ESI.†

Nomenclature

AFEX	Ammonia fiber expansion
ASGH	AFEX-pretreated switchgrass hydrolysate
CB	Combustor & boiler
ESI	Electronic supplementary information
FERM	Fermentation
GGE	Gasoline gallon equivalent
GVL	γ-Valerolactone
HYD	Hydrolysis
IBA	Isobutanol
MFSP	Minimum fuel selling price
SEP	Separations
TBG	Turbogenerator
TEA	Technoeconomic analysis
WWT	Wastewater treatment

Data availability

The data supporting this article has been included as part of the ESI.† Table S1† shows details of the experimental results. Section S4† gives the details of the optimization model. Tables S3 to S5† show the parameters used in the optimization model.

Author contributions

AEPL: conceptualization, data curation, formal analysis, investigation, methodology, resources, software, validation, visualization, writing – original draft, writing – review & editing. JC: conceptualization, data curation, investigation, methodology, resources, validation, writing – review & editing. LCA: resources, writing – review & editing. TKS: conceptualization, investigation, methodology, funding acquisition, validation, writing – review & editing. YZ: conceptualization, data curation, investigation, methodology, resources, funding acquisition, validation, writing – review & editing. SDK: conceptualization, data curation, investigation, methodology, resources, funding acquisition, validation, writing – review & editing. CTH: conceptualization, funding acquisition, methodology, project administration, supervision, validation, writing – review & editing. CTM: conceptualization, formal analysis, funding acquisition, investigation, methodology, project administration, supervision, validation, writing – review & editing.

Conflicts of interest

Strain BTX1858 is a proprietary strain made available to researchers under a Material Transfer Agreement with Butamax Advanced Biofuels, LLC, who retains all rights to the strain. LA is an employee of IFF and formerly of Butamax Advanced Biofuels, LLC.

Acknowledgements

We thank Butamax and DuPont R&D for designing and providing the industrial strain BTX1858, as well as Novozymes for providing NS 22257 (Cellulase) and NS 22244 (Xylanase) enzymes. We thank Jose Serate, Dan Xie, and Evan Handowski for performing fermentations and Mick McGee and the GLBRC Metabolomics Facility for HPLC-RID and Gas Chromatography analyses. Cliff Foster and the GLBRC Biomass Analytics Facility performed the compositional analysis of the untreated feedstocks. This material is based upon work supported in part by the Great Lakes Bioenergy Research Center, U.S. Department of Energy, Office of Science, Office of Biological and Environmental Research under Award Number DE-SC0018409. Research in the Hittinger Lab is also supported by the National Science Foundation under Grant No. DEB-2110403, the USDA National Institute of Food and Agriculture (Hatch Project 7005101), and an H. I. Romnes Faculty Fellowship, supported by the Office of the Vice Chancellor for Research and Graduate Education with funding from the Wisconsin Alumni Research Foundation.

References

1 R. Sindhu, P. Binod, A. Pandey, S. Ankaram, Y. Duan and M. K. Awasthi, in *Current Developments in Biotechnology and Bioengineering*, ed. S. Kumar, R. Kumar and A. Pandey, Elsevier, 2019, pp. 79–92.
2 R. Muñoz, J. B. Montón, M. C. Burguet and J. de la Torre, *Sep. Purif. Technol.*, 2006, **50**, 175–183.
3 K. Breitkreuz, A. Menne and A. Kraft, *Biofuels, Bioprod. Biorefin.*, 2014, **8**, 504–515.
4 J. D. Taylor, M. M. Jenni and M. W. Peters, *Top. Catal.*, 2010, **53**, 1224–1230.
5 M. C. Al-Kinany, S. A. Al-Drees, H. A. Al -Megren, S. M. Alshihri, E. A. Alghilan, F. A. Al-Shehri, A. S. Al-Hamdan, A. J. Alghamdi and S. D. Al-Dress, *Appl. Petrochem. Res.*, 2019, **9**, 35–45.
6 A. V. Lavrenov, T. R. Karpova, E. A. Buluchevskii and E. N. Bogdanets, *Catal Ind*, 2016, **8**, 316–327.
7 Y. Su, W. Zhang, A. Zhang and W. Shao, *Appl. Sci.*, 2020, **10**, 8222.
8 P. P. Peralta-Yahya, F. Zhang, S. B. Del Cardayre and J. D. Keasling, *Nature*, 2012, **488**(7411), 320–328.
9 A. R. Mankar, A. Pandey, A. Modak and K. K. Pant, *Bioresour. Technol.*, 2021, **334**, 125235.
10 W. Won, A. H. Motagamwala, J. A. Dumesic and C. T. Maravelias, *React. Chem. Eng.*, 2017, **2**, 397–405.
11 J. Han, J. S. Luterbacher, D. M. Alonso, J. A. Dumesic and C. T. Maravelias, *Bioresour. Technol.*, 2015, **182**, 258–266.
12 I. T. Horváth, H. Mehdi, V. Fábos, L. Boda and L. T. Mika, *Green Chem.*, 2008, **10**, 238–242.
13 J. S. Luterbacher, J. M. Rand, D. M. Alonso, J. Han, J. T. Youngquist, C. T. Maravelias, B. F. Pfleger and J. A. Dumesic, *Science*, 2014, **343**, 277–280.
14 A. H. Motagamwala, W. Won, C. T. Maravelias and J. A. Dumesic, *Green Chem.*, 2016, **18**, 5756–5763.
15 Y. S. Jang, J. Yang, J. K. Kim, T. I. Kim, Y.-C. Park, I. J. Kim and K. H. Kim, *Biotechnol. J.*, 2023, 2300270.
16 K. Kuroda, S. K. Hammer, Y. Watanabe, J. Montaño López, G. R. Fink, G. Stephanopoulos, M. Ueda and J. L. Avalos, *Cell Syst.*, 2019, **9**, 534–547.e5.
17 M. Sardi, M. Krause, J. Heilberger and A. P. Gasch, *G3: Genes, Genomes, Genet.*, 2018, **8**, 3881–3890.
18 C. Fu, Z. Li, C. Jia, W. Zhang, Y. Zhang, C. Yi and S. Xie, *Energy Convers. Manage.: X*, 2021, **10**, 100059.
19 A. Roussos, N. Misailidis, A. Koulouris, F. Zimbardi and D. Petrides, *Processes*, 2019, **7**, 667.
20 F. V. Gambacorta, E. R. Wagner, T. B. Jacobson, M. Tremaine, L. K. Muehlbauer, M. A. McGee, J. J. Baerwald, R. L. Wrobel, J. F. Wolters, M. Place, J. J. Dietrich, D. Xie, J. Serate, S. Gajbhiye, L. Liu, M. Vang-Smith, J. J. Coon, Y. Zhang, A. P. Gasch, D. Amador-Noguez, C. T. Hittinger, T. K. Sato and B. F. Pfleger, *Synth. Syst. Biotechnol.*, 2022, **7**, 738–749.
21 Y. Zhang, S. Lane, J. M. Chen, S. K. Hammer, J. Luttinger, L. Yang, Y. S. Jin and J. L. Avalos, *Biotechnol. Biofuels*, 2019, **12**, 1–15.

22 X. Chen, K. F. Nielsen, I. Borodina, M. C. Kielland-Brandt and K. Karhumaa, *Biotechnol. Biofuels*, 2011, **4**, 1–12.
23 F. Matsuda, J. Ishii, T. Kondo, K. Ida, H. Tezuka and A. Kondo, *Microb. Cell Fact.*, 2013, **12**, 119.
24 I. N. Ghosh, J. Martien, A. S. Hebert, Y. Zhang, J. J. Coon, D. Amador-Noguez and R. Landick, *Metab. Eng.*, 2019, **52**, 324–340.
25 R. Liu, F. Zhu, L. Lu, A. Fu, J. Lu, Z. Deng and T. Liu, *Metab. Eng.*, 2014, **22**, 10–21.
26 S. Atsumi, T. Hanai and J. C. Liao, *Nature*, 2008, **451**, 86–89.
27 Y. Liu, I. N. Ghosh, J. Martien, Y. Zhang, D. Amador-Noguez and R. Landick, *Metab. Eng.*, 2020, **61**, 261–274.
28 H. M. Jung, J. Y. Lee, J. H. Lee and M. K. Oh, *Bioresour. Technol.*, 2018, **259**, 373–380.
29 J. J. Minty, M. E. Singer, S. A. Scholz, C. H. Bae, J. H. Ahn, C. E. Foster, J. C. Liao and X. N. Lin, *Proc. Natl. Acad. Sci. U. S. A.*, 2013, **110**, 14592–14597.
30 G. M. Rubinstein, G. L. Lipscomb, A. M. Williams-Rhaesa, G. J. Schut, R. M. Kelly and M. W. W. Adams, *J. Ind. Microbiol. Biotechnol.*, 2020, **47**, 585–597.
31 B. Blombach, T. Riester, S. Wieschalka, C. Ziert, J. W. Youn, V. F. Wendisch and B. J. Eikmanns, *Appl. Environ. Microbiol.*, 2011, **77**, 3300–3310.
32 S. Bastian, X. Liu, J. T. Meyerowitz, C. D. Snow, M. M. Y. Chen and F. H. Arnold, *Metab. Eng.*, 2011, **13**, 345–352.
33 H. Cai, J. Markham, S. Jones, P. T. Benavides, J. B. Dunn, M. Biddy, L. Tao, P. Lamers and S. Phillips, *ACS Sustain. Chem. Eng.*, 2018, **6**, 8790–8800.
34 L. Tao, E. C. D. Tan, R. Mccormick, M. Zhang, A. Aden, X. He and B. T. Zigler, *Biofuels, Bioprod. Biorefin.*, 2014, **8**, 30–48.
35 A. E. Pastore de Lima, R. L. Wrobel, B. Paul, L. C. Anthony, T. K. Sato, Y. Zhang, C. T. Hittinger and C. T. Maravelias, *Sustainable Energy Fuels*, 2023, **7**, 3266–3275.
36 F. Kerkel, M. Markiewicz, S. Stolte, E. Müller and W. Kunz, *Green Chem.*, 2021, **23**, 2962–2976.
37 I. Gelfand, S. K. Hamilton, A. N. Kravchenko, R. D. Jackson, K. D. Thelen and G. P. Robertson, *Environ. Sci. Technol.*, 2020, **54**, 2961–2974.
38 N. L. Haan, G. N. M. Benucci, C. M. Fiser, G. Bonito and D. A. Landis, *Sci. Adv.*, 2023, **9**, eadh7960.
39 J. Piotrowski, Y. Zhang, T. Sato, I. Ong, D. Keating, D. Bates and R. Landick, *Front. Microbiol.*, 2014, **5**, 1–8.
40 D. M. Alonso, S. H. Hakim, S. Zhou, W. Won, O. Hosseinaei, J. Tao, V. Garcia-Negron, A. H. Motagamwala, M. A. Mellmer, K. Huang, C. J. Houtman, N. Labbé, D. P. Harper, C. T. Maravelias, T. Runge and J. A. Dumesic, *Sci. Adv.*, 2017, **3**, e1603301.
41 D. Humbird, R. Davis, L. Tao, C. Kinchin, D. Hsu, A. Aden, P. Schoen, J. Lukas, B. Olthof, M. Worley, D. Sexton and D. Dudgeon, *Process Design and Economics for Conversion of Lignocellulosic Biomass to Ethanol*, 2011.
42 F. K. Kazi, J. Fortman, R. Anex, G. Kothandaraman, D. Hsu, A. Aden and A. Dutta, *Techno-Economic Analysis of Biochemical Scenarios for Production of Cellulosic Ethanol Techno-Economic Analysis of Biochemical Scenarios for Production of Cellulosic Ethanol*, Golden, Colorado, 2010.
43 A. Aden, M. Ruth, K. Ibsen, J. Jechura, K. Neeves, J. Sheehan, B. Wallace, L. Montague, A. Slayton and J. Lukas, *Lignocellulosic Biomass to Ethanol Process Design and Economics Utilizing Co-current Dilute Acid Prehydrolysis and Enzymatic Hydrolysis for Corn Stover*, Golden, Colorado, 2002.
44 K. Huang, P. Fasahati and C. T. Maravelias, *iScience*, 2020, **23**, 100751.
45 R. T. L. Ng, P. Fasahati, K. Huang and C. T. Maravelias, *Appl. Energy*, 2019, **241**, 491–503.
46 A. R. C. Morais, J. Zhang, H. Dong, W. G. Otto, T. Mokomele, D. Hodge, V. Balan, B. E. Dale, R. M. Lukasik and L. da Costa Sousa, *Green Chem.*, 2022, **24**, 4443–4462.
47 L. G. Oates, D. S. Duncan, G. R. Sanford, C. Liang and R. D. Jackson, *Agric., Ecosyst. Environ.*, 2016, **233**, 396–403.
48 C. E. Foster, T. M. Martin and M. Pauly, *JoVE*, 2010, e1837.
49 J. M. Perez, C. Sener, S. Misra, G. E. Umana, J. Coplien, D. Haak, Y. Li, C. T. Maravelias, S. D. Karlen, J. Ralph, T. J. Donohue and D. R. Noguera, *Green Chem.*, 2022, **24**, 2795–2811.
50 A. Sluiter, B. Hames, R. Ruiz, C. Scarlata, J. Sluiter, D. Templeton and D. Crocker, *Determination of Structural Carbohydrates and Lignin in Biomass*, 2012.
51 A. P. Mariano, M. J. Keshtkar, D. I. P. Atala, F. M. Filho, M. R. W. MacIel, R. M. I. Filho and P. Stuart, *Energy Fuels*, 2011, **25**, 2347–2355.